Xenon

DOI: 10.1002/anie.200701688

The Blue Xe_4^+ Cation: Experimental Detection and Theoretical Characterization**

Stefan Seidel, Konrad Seppelt, Christoph van Wüllen,* and Xiao Ying Sun*

Xenon cations can be considered the most simple compounds of this rare gas. Historically, the transient existence of a Xe^+ ion in the reaction between Xe and PtF_6 marked the beginning of noble-gas chemistry.[1] Later, the Xe_2^+ ion was obtained, which is by now well-characterized, including by a single crystal structure determination on $Xe_2^+Sb_4F_{21}^-$.[2] The striking feature of this cation is its intense green color, which stems from an absorption in the red (705–715 mm).

In molecular beam experiments, a large number of Xe_n^+ ions with $n \leq 30$ can be detected by means of mass spectrometry.[3] The structures of such cationic clusters have been predicted by various calculations.[3,4] The salient feature of such clusters is a delocalization of the charge over a small trimeric or tetrameric core held together by covalent bonds, while the other xenon atoms are attached to this core by induction forces.[3]

We have now observed that the green Xe_2^+ ion converts into a dark blue solution in excess, pure SbF_5 if a xenon pressure of about 30–50 bar is applied. Under these conditions the solvent is a homogenous mixture of SbF_5 and liquid Xe. The color change from green to blue is reversible if the xenon pressure is reduced, which is most simply done by cooling the sample. At present it seems hopeless to grow single crystals, owing to the fact that highly viscous SbF_5 seems to be the only appropriate solvent.

Cooling below room temperature leads to loss of the blue color because of reduction of the autogenous xenon pressure. The presence of SbF_5 is essential because of its extreme Lewis acidity, which prevents the formation of more basic anions, such as SbF_6^-. No other solvent for this reaction has been found to date. Therefore, the characterization of the blue material is based only on spectroscopic data, guided by theoretical calculations.

The absorption spectrum of the blue material is shown in Figure 1. Three bands are observed at 370, 620 (broad), and 800 nm, leaving only the blue region transparent. Figure 1 also shows the narrower, different absorption spectra of green

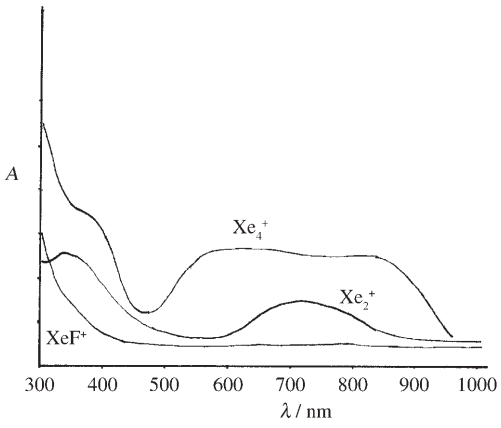

Figure 1. Absorption spectrum of XeF^+, Xe_2^+ and Xe_4^+.

the Xe_2^+ ion. The Raman spectrum of the blue compound has a strong band at 110 cm^{-1} (Figure 2) along with the usual Sb–F vibrations around 250 and 700 cm^{-1}.[5] Although the

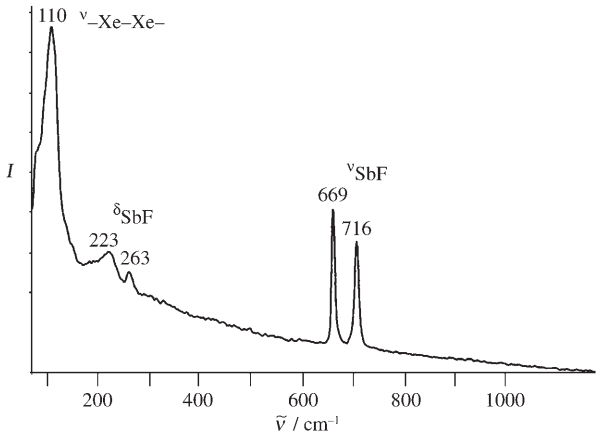

Figure 2. Raman spectrum of Xe_4^+ in SbF_5/Xe solution. The band at 223 cm^{-1} might be, in part, the first overtone of the 110 cm^{-1} band as well as δ_{SbF} of SbF_5.

observed signal is quite close to the stretching vibration of the Xe_2^+ ion at 123 cm^{-1}, the two Raman bands can be clearly differentiated. The IR spectrum shows no band in the region between 60 and 180 cm^{-1}, in spite of a 1-mm path length and a high concentration of the blue compound. Not surprisingly, no EPR signal is detected at room temperature. This finding is similar to the case of the Xe_2^+ ion, which is only EPR-active at temperatures less than or equal to 5 K. Also, in the ^{129}Xe NMR spectrum, no signal other than that of elemental xenon can be observed.

[*] Dr. S. Seidel, Prof. Dr. K. Seppelt
Institut für Chemie und Biochemie
Freie Universität Berlin
Fabeckstrasse 34–36, 14195 Berlin (Germany)
Fax: (+49) 30-8385-3310
E-mail: seppelt@chemie.fu-berlin.de
Prof. Dr. C. van Wüllen, X. Y. Sun
Technische Universität Berlin
Strasse des 17. Juni 135, 10623 Berlin (Germany)
Fax: (+49) 30-3142-3727
E-mail: christoph.vanwuellen@tu-berlin.de

[**] This work was supported by the Deutsche Forschungsgemeinschaft and the Fonds der Chemischen Industrie.

We have considered the following cationic xenon species as candidates for the cause of the blue color: Xe_3^{2+}, Xe_3^{+}, and Xe_4^{+}. We have undertaken high-level ab initio calculations with large basis sets and inclusion of spin–orbit coupling (see Computational Details). Computed molecular structures are summarized in Table 1, reaction and ionization energies in Table 2, and UV/Vis absorptions in Table 3. The calculations reproduce the experimental data on the Xe_2^{+} ion very well: $R_e = 309.8$ (exptl 308.7(1)) pm, $\omega_e = 126$ (exptl 123) cm^{-1}.[2]

Of the three species considered as candidates for the blue compound, the Xe_3^{2+} ion is chemically the most attractive, since it is isoelectronic to the well-known I_3^{-} ion. It can be ruled out, however, for three reasons: 1) The calculated vibrational spectra do not agree with the experiment. 2) It should spontaneously decompose in the presence of excess Xe into Xe_2^{+} (see the calculated energetics in Table 2). 3) Formation of the Xe_3^{2+} ion would need a strong oxidizer, and the only one that could be in the system would be XeF^{+} from the original preparation of the Xe_2^{+} ion. However, the XeF^{+} ion is totally absent, as its very strong and characteristic Raman line at 600–620 cm^{-1} is missing at all xenon pressures.

The Xe_3^{+} ion is a difficult problem from a theoretical viewpoint. MRCI (multireference configuration interaction) calculations including spin–orbit effects find a clear preference for a linear geometry over a triangular (C_{2v}) arrangement,[4] but the linear, symmetric ($D_{\infty h}$) structure can be easily distorted to a linear, asymmetric ($C_{\infty v}$) one. While we actually find a $C_{\infty v}$ structure at the Hartree–Fock level, inclusion of electron correlation always favors the higher-symmetry $D_{\infty h}$ geometry as the overall minimum, in agreement with previous theoretical investigations.[4] For the symmetric structure, the calculated symmetric stretching frequency does not agree with the experimental value in the Raman spectrum (see Table 1), and the expected asymmetric stretching vibration (in the IR spectrum) is not observed at all in the experiment. It is thus not likely that Xe_3^{+} units are present under experimental conditions.

For the Xe_4^{+} ion, semiempirical calculations[4d] report two low-lying isomers, namely a symmetric ($D_{\infty h}$) linear structure which can be described as a Xe_2^{+} core with two weakly (end-on) bound Xe atoms, and a T-shaped structure that is essentially a weakly perturbed linear Xe_3^{+} ion with a neutral Xe atom loosely attached to the central atom and one of the terminal atoms. Our scalar-relativistic MP2 (second-order Møller–Plesset perturbation theory) calculations find the same structures with virtually the same energy. The T-shaped Xe_4^{+} ion (in which the neutral Xe atom is attached to two of the Xe atoms of a trimeric core by bond lengths of 430 and 448 pm) has vibrational spectra very close to those of the Xe_3^{+} ion and can be ruled out for the same reasons. Therefore, we concentrated on linear ($D_{\infty h}$) Xe_4^{+}, whose bond lengths (320 and 357 pm) indicate that all four atoms are held together by covalent bonds rather than induction forces. The calculated frequencies fit the Raman spectrum well (110.9 vs. 110 cm^{-1} for the stretching of the central Xe^{2+} unit); all other frequencies are predicted to be found below the detection limits of 60 cm^{-1} in our Raman and IR setups. The overall chemical reaction is given in Equation (1):

$$XeF^{+}Sb_2F_{11}^{-} + 3\,Xe \xrightarrow{SbF_5} 2\,Xe_2^{+}Sb_xF_{5x+1}^{-} \xrightarrow{4\,Xe} 2\,Xe_4^{+}Sb_xF_{5x+1}^{-} \qquad (1)$$

Calculated optical excitations in the UV/Vis region are shown in Table 3. Comparison with the experimentally known spectra of the Xe_2^{+} and Xe_3^{+} ions show fair agreement, with a tendency to overestimate the excitation energy for the transition with the highest wavelength. Note, however, that a discrepancy such as 665 versus 715 nm means that the energy of the excited state is overestimated by merely 0.13 eV. The question arises as to whether gas-phase calculations should be compared with condensed-phase measurements. This approach is justified, since for the UV transition of the

Table 1: Calculated equilibrium bond lengths and harmonic vibrational symmetric and antisymmetric stretching frequencies of linear $D_{\infty h}$ structures of Xe_2^{+}, Xe_3^{+}, Xe_3^{2+}, and Xe_4^{+}.

	R_e [pm]		ω_e^{s} [cm^{-1}]		ω_e^{as} [cm^{-1}]	
Xe_2^{+}	(310.7)[a]	309.8[b]	(127.9)[a]	126.0[b]	–	–
Xe_3^{+}	(327.2)	326.3	(76.4)	73.2	(72.0)[a]	72.6[b]
Xe_3^{2+}	(292.4)	295.1	(102.9)	90.2	(179.2)	171.2
Xe_4^{+}	(320.4)	319.0	(101.9)	110.9	(41.5)	n.c.[c]
	(366.8)	352.9	(31.1)	43.0		

[a] Scalar relativistic MP2 calculation, cc-pVTZ basis set. [b] CCSD(T) calculation, VQZ basis set, spin orbit effects taken from MRCI calculations. [c] Not calculated.

Table 2: Reaction and ionization energies (ΔE [eV]).[a]

			ΔE_{calcd}	ΔE_{exptl}
Xe	$\xrightarrow{-e^-}$	Xe^{+}	12.17	12.13[b]
$Xe^{+} + Xe$	$\rightarrow$	Xe_2^{+}	−0.99	−1.03[c]
$Xe_2^{+} + Xe$	$\rightarrow$	Xe_3^{+}	−0.32	−0.27[d]
Xe_3^{+}	$\xrightarrow{-e^-}$	Xe_3^{2+}	14.94	
Xe_3^{2+}	$\xrightarrow{-e^-}$	$Xe_2^{2+} + Xe^{+}$	−2.45	
$Xe_3^{2+} + Xe$	$\rightarrow$	$2\,Xe_2^{+}$	−3.47	
$Xe_3^{+} + Xe$	$\rightarrow$	Xe_4^{+} (D_{8h})	−0.16	

[a] CCSD(T) results augmented by spin orbit effects from MRCI calculations, without zero point vibrational corrections, which are estimated to ca. 0.01 eV from MP2 results. The CCSD(T) results have been extrapolated to the basis set limit and include BSSE corrections. Experimental values, where available, are given for comparison. [b] Ref. [7]. [c] Ref. [8]. [d] Ref. [9]

Table 3: Calculated vertical UV/Vis excitations, wavelengths (λ [nm]), transition moments ($||\vec{\mu}||$) in atomic units, and (dimensionless) oscillator strengths (f).[a]

		λ		$||\vec{\mu}||$	f
Xe_2^{+}	$I(\frac{1}{2})_u \rightarrow I(\frac{1}{2})_g$	665	(715)[b]	1.21	0.067
	$I(\frac{1}{2})_u \rightarrow II(\frac{1}{2})_g$	327	(335)[b]	2.17	0.436
Xe_3^{+}	$I(\frac{1}{2})_u \rightarrow I(\frac{1}{2})_g$	611	(709)[c]	3.58	0.636
	$I(\frac{1}{2})_u \rightarrow II(\frac{1}{2})_g$	387	(397)[c]	1.64	0.212
Xe_4^{+}	$I(\frac{1}{2})_u \rightarrow I(\frac{1}{2})_g$	719	(800)[d]	4.55	0.875
	$I(\frac{1}{2})_u \rightarrow II(\frac{1}{2})_g$	559	(620)[d]	0.19	0.002
	$I(\frac{1}{2})_u \rightarrow III(\frac{1}{2})_g$	387	(380)[d]	1.17	0.108
	$I(\frac{1}{2})_u \rightarrow IV(\frac{1}{2})_g$	282		0.49	0.025

[a] Experimental values in parentheses. MRCI + spin orbit CI, V5Z basis set, only valence electrons included in the correlation treatment. [b] Ref. [2]. [c] Ref. [3]. [d] This work.

Xe_2^+ ion, at least, experiments in the condensed phase[2c] and in the gas phase[6] have almost the same absorption wavelengths (335 and 340 nm). For the Xe_4^+ ion, the calculations find three bands in the visible region and one UV band. Considerable vibrational broadening can be expected, since the transition energy depends strongly on the length of the outer Xe–Xe bond, which is a rather floppy mode. Two of the transitions (at 559 and 282 nm) are considerably weaker than the others, which is inconsistent with the experimental observation. Further calculations show that upon stretching of the weak and long Xe–Xe bonds, these two transitions (at 559 and 282 nm) become local excitations of the Xe_2^+ core, while the other two become charge-transfer transitions (at about 718 and 427 nm, split by the spin–orbit splitting of the Xe^+ ion). At the same time, the intensity of the local excitations increases while the intensity of the charge-transfer excitations vanishes with the overlap of the neutral Xe atoms with the ionic dimer core.

While we present evidence that the Xe_4^+ ion with $D_{\infty h}$ structure is the cause of the blue species, we cannot rule out that under the experimental conditions higher xenon aggregates $Xe_4^+ \cdot Xe_n$ are formed in which the surrounding additional xenon atoms are very loosely bound. Such large cationic clusters are formed under molecular-beam conditions. Kalus et al. have calculated that 12–18 additional xenon atoms are needed to stabilize a linear symmetric Xe_4^+ unit, with the outer xenon atoms at a distance of about 440 pm from the Xe_4^+ core.[4d–f] UV/Vis spectra of those clusters in the molecular beam experiment indeed show a bathochromic shift of the absorption with increasing size of the cluster. Interestingly, higher Xe_n^+ aggregates could be broken apart by photo decomposition, leaving behind a Xe_4^+ ion fragment that is assigned a linear structure.[3] Figure 3 shows the structure of Xe_4^+ according to our calculations.

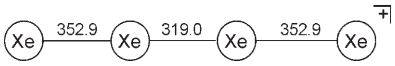

Figure 3. Structure of the Xe_4^+ ion ($D_{\infty h}$) according to our calculations (bond lengths in pm).

Experimental Section

Yellow $XeF^+Sb_2F_{11}^-$ was obtained by dissolving XeF_2 in a threefold excess of SbF_5, preferably in a PFA (poly(perfluorovinylether-*co*-tetrafluoroethene)) tube, and subsequent pumping to dryness.[10] Liquid samples of $Xe_4^+Sb_xF_y^-$ were prepared by adding an excess (ca. five-fold) of SbF_5 onto $XeF^+Sb_2F_{11}^-$ and condensing a large excess of xenon onto the mixture so that the total volume was doubled. For each physical measurement (Raman, IR, UV/Vis, EPR, ^{129}Xe NMR) a special sample was made, most often a thick-walled glass capillary with an inner diameter of 1–2 mm. The IR experiment was done in a small stainless steel cell with 1 mm thick PFA or prefluorinated polyethylene windows.

SbF_5 dissolved easily in liquid xenon, thus raising the boiling point of the xenon above room temperature, well above its critical point at 16.6 °C. The pressures in our samples can be estimated to be near the critical pressure of 54.2 bar. If only a little xenon is applied, for example, 1–3 bar, then the solution remains deep green (Xe_2^+).[2] Standard equipment was used for the various physical measurements.

Computational details: Quantum chemical calculations have been performed using an effective core potential (ECP) for Xe that replaces the inner 1s to 3d electrons of Xe.[11] Polarized correlation-consistent basis sets of triple- through quintuple-zeta quality (cc-pVxZ-PP with x = T,Q,5[11]) were used and are referred to as VTZ, VQZ, and V5Z. Calculations including electron correlation (MP2, coupled-cluster (CCSD(T)), and MRCI methods) either correlate only the valence electrons (from the Xe 5s5p atomic shells) or include the subvalence 4d electrons. The basis sets are not well-suited to treat core correlation, which leads to a slight overestimation of the binding energies. MP2 and CCSD(T) were performed on top of a spin-restricted Hartree–Fock calculation, while internally contracted MRCI calculations[12] use CASSCF (complete active space self-consistent field) orbitals optimized for a weighted average of states. The active space includes the full valence space (5s, 5p of Xe).

For geometry optimizations and frequency calculations, a large weight (80 %) is used for the $^2\sum_u^+$ ground state, while the lowest $^2\prod_u$ state is included with 20 % weight. Such a procedure usually improves the description of weakly occupied active orbitals. In the present calculations, all valence orbitals are significantly occupied anyway, so the choice of the weights only weakly affects the calculated spin–orbit effects. To calculate optical excitations, all valence states are included in the state-averaged CASSCF calculation with equal weight. Spin–orbit coupling is taken into account by a spin–orbit CI.[13] For geometry optimizations, we included the ungerade valence states of the monocations (Xe_2^+, Xe_3^+, Xe_4^+), and for Xe_3^{2+}, we included the $^1\sum_g^+$ ground state, the next $^1\sum_g^+$ and two $^3\prod_g$ states. The calculation of optical excitations involved all valence states in the spin–orbit CI. CCSD(T), CASSCF, MRCI, and spin–orbit CI single-point calculations were performed with the Molpro[14] program, and spin-unrestricted MP2 results (VTZ basis set) were obtained with the Gaussian (G03) program.[15] The computed minimum structures have been characterized by a vibrational analysis based on analytical second derivatives. Since electron correlation beyond MP2 and spin–orbit coupling have an opposite effect on bond lengths and vibrational frequencies, these calculations can be used to give a first overview. Further investigations will concentrate on structures of $D_{\infty h}$ symmetry. CCSD(T) energies with the VQZ basis set (valence and subvalence electrons correlated) have been augmented by spin–orbit energy lowerings (ΔSO) from spin–orbit CI calculations with MRCI wave functions (ΔSO is the energy difference between the lowest eigenvalue and the lowest diagonal element of the spin–orbit CI matrix). In the MRCI calculations, only the valence electrons were correlated, but we have checked that this situation only marginally affects ΔSO. For the Xe_2^+ ion, the minimum geometry and the frequency of the Raman-active (fully symmetric) mode have been calculated by a polynomial fit to about ten data points. For the Xe_3^+, Xe_3^{2+}, and Xe_4^+ ions, a quadratic fit was done on a 7×7 grid of data points using two coordinates, such that we get the symmetric and asymmetric stretching frequencies for the triatomic ions but only the two symmetric stretching frequencies for the tetratomic ion. Energy differences (ionization and reaction energies) have been calculated by single-point calculations at the CCSD(T) + ΔSO level with an extrapolation to the basis-set limit[16] based on calculations with the VQZ and V5Z basis sets, and with a counterpoise correction[17] for the basis-set superposition effect.

Received: April 17, 2007
Published online: July 31, 2007

Keywords: ab initio calculation · cations · structure elucidation · xenon

[1] N. Bartlett, *Proc. Chem. Soc.* **1962**, 218; L. Graham, O. Graudejus, N. K. Jha, N. Bartlett, *Coord. Chem. Rev.* **2000**, *197*, 321 – 334.

[2] L. Stein, J. R. Norris, A. J. Downs, A. R. Miniham, *J. Chem. Soc. Chem. Commun.* **1978**, 502 – 504; L. Stein, W. W. Henderson, *J. Am. Chem. Soc.* **1980**, *102*, 2856 – 2857; D. R. Brown, J. M. Clegg, A. J. Downs, R. C. Fowler, A. R. Miniham, J. R. Norris, L. Stein, *Inorg. Chem.* **1992**, *31*, 5041 – 5052; T. Drews, K. Seppelt, *Angew. Chem.* **1997**, *109*, 264 – 266; *Angew. Chem. Int. Ed. Engl.* **1997**, *36*, 273 – 274.

[3] H. Haberland, B. v. Issendorf, T. Kolar, H. Kornmeier, C. Ludewigt, A. Risch, *Phys. Rev. Lett.* **1991**, *67*, 3290 – 3293; B. von Issendorf, A. Hofmann, H. Haberland, *J. Chem. Phys.* **1999**, *111*, 2513 – 2518; J. A. Gascon, R. W. Hall, C. Ludewigt, H. Haberland, *J. Chem. Phys.* **2002**, *117*, 8391 – 8403.

[4] a) S. D. Peyerimhoff, *Z. Phys. D* **1990**, *15*, 161 – 169; b) M. Daskalopoulou, H.-K. Böhmer, I. Last, T. F. George, *J. Chem. Phys.* **1990**, *93*, 8925 – 8938; c) N. L. Doltsinis, *Mol. Phys.* **1999**, *97*, 847 – 852; d) R. Kalus, D. Hrivňák, *Chem. Phys.* **2002**, *278*, 21 – 29; e) P. Paška, D. Hrivňák, R. Kalus, *Chem. Phys.* **2003**, *286*, 237 – 248; f) R. Kalus, D. Hrivňák, P. Paška, *Chem. Phys.* **2005**, *311*, 287 – 297.

[5] J. Gaunt, J. B. Ainscough, *Spectrochim. Acta* **1957**, *10*, 57 – 60.

[6] A. W. McCown, M. N. Ediger, J. G. Eden, *Phys. Rev. A* **1983**, *28*, 3362 – 3370.

[7] NIST Atomic Spectra Database, http://physics.nist.gov/PhysRefData/ASD.

[8] P. M. Dehmer, J. L. Dehmer, *J. Chem. Phys.* **1978**, *68*, 3462 – 3470.

[9] H. Helm, *Phys. Rev. Lett.* **1991**, *67*, 3290 – 3293.

[10] V. M. McRae, R. D. Peacock, D. R. Russell, *Chem. Commun.* **1969**, *62*.

[11] K. A. Peterson, D. Figgen, E. Goll, H. Stoll, M. Dolg, *J. Chem. Phys.* **2003**, *119*, 11113 – 11123.

[12] a) H.-J. Werner, P. J. Knowles, *J. Chem. Phys.* **1988**, *89*, 5803 – 5814; b) P. J. Knowles, H.-J. Werner, *Chem. Phys. Lett.* **1988**, *145*, 514 – 522.

[13] R. Pitzer, N. Winter, *J. Phys. Chem.* **1988**, *92*, 3061 – 3063.

[14] H.-J. Werner et al., Molpro, version 2002.6, a package of ab initio programs, 2002, see http://www.molpro.net.

[15] Gaussian 03, Revision B.04, M. J. Frisch, G. W. Trucks, H. B. Schlegel, G. E. Scuseria, M. A. Robb, J. R. Cheeseman, J. A. Montgomery, Jr., T. Vreven, K. N. Kudin, J. C. Burant, J. M. Millam, S. S. Iyengar, J. Tomasi, V. Barone, B. Mennucci, M. Cossi, G. Scalmani, N. Rega, G. A. Petersson, H. Nakatsuji, M. Hada, M. Ehara, K. Toyota, R. Fukuda, J. Hasegawa, M. Ishida, T. Nakajima, Y. Honda, O. Kitao, H. Nakai, M. Klene, X. Li, J. E. Knox, H. P. Hratchian, J. B. Cross, C. Adamo, J. Jaramillo, R. Gomperts, R. E. Stratmann, O. Yazyev, A. J. Austin, R. Cammi, C. Pomelli, J. W. Ochterski, P. Y. Ayala, K. Morokuma, G. A. Voth, P. Salvador, J. J. Dannenberg, V. G. Zakrzewski, S. Dapprich, A. D. Daniels, M. C. Strain, O. Farkas, D. K. Malick, A. D. Rabuck, K. Raghavachari, J. B. Foresman, J. V. Ortiz, Q. Cui, A. G. Baboul, S. Clifford, J. Cioslowski, B. B. Stefanov, G. Liu, A. Liashenko, P. Piskorz, I. Komaromi, R. L. Martin, D. J. Fox, T. Keith, M. A. Al-Laham, C. Y. Peng, A. Nanayakkara, M. Challacombe, P. M. W. Gill, B. Johnson, W. Chen, M. W. Wong, C. Gonzalez, J. A. Pople, Gaussian, Inc., Pittsburgh PA, **2003**.

[16] A. Halkier, T. Helgaker, P. Jorgensen, W. Klopper, H. Koch, J. Olsen, A. K. Wilson, *Chem. Phys. Lett.* **1998**, *286*, 243 – 252.

[17] S. F. Boys, F. Bernardi, *Mol. Phys.* **1970**, *19*, 553 – 566.

